Wood Liquefaction and its Application to Novolac Resin

Hui Pan[1], Chung-Yun Hse[2] and Todd F. Shupe[3]
[1]Calhound Research Station, Louisiana State University AgCenter, Calhoun, LA, 71225, USA
[2]USDA Forest Service, Southern Experiment Station, Pineville, LA 71360, USA
[3]School of Renewable Natural Resources, Louisiana State University, Baton Rouge, LA 70803, USA

Abstract

Wood liquefaction was conducted using phenol as a reagent solvent with a weak acid catalyst in two different reactors: (Alma et al., 1995a.) an atmospheric glass reactor and (Alma et al., 1995b.) a sealed Parr® reactor. Residues were characterized by wet chemical analyses, Fourier transform infrared (FT-IR) spectroscopy, and X-ray diffraction (XRD). The FT-IR spectra of the liquefied wood residues showed a peak at 1735 cm^{-1}, which was attributed to the ester carbonyl group in xylan, disappeared in the spectrum of the residue from liquefied wood under a sealed reaction system, indicating different liquefaction mechanisms of the liquefaction reactions conducted in the atmospheric glass reactor versus sealed metal reactor. The crystallinity index of the liquefied wood residues was higher than that of the original wood particles. Two different liquefied wood/phenol/formaldehyde (LWPF) resins were synthesized from liquefied wood reacted in an atmospheric glass reactor (LWPF-A) and a sealed metal reactor (LWPF-B). The onset cure temperature of LWPF-A resin was higher than LWPF-B while the peak temperatures of these two resins were close. The activation energies of two LWPF resins were similar to each other and to a lignin-phenol-formaldehyde resin. However, they both were higher than a typical phenol-formaldehyde resin. The compression molded panels made with LWPF-A resin performed better physical and mechanical properties than that made with LWPF-B resin.

Introduction

Wood liquefaction using phenol as a reagent solvent has long been studied as a novel technique to utilize biomass for chemicals and improve the thermofluidity and processibility of wood. Liquefaction reactions can be conducted without a catalyst at an elevated temperature around 250°C or with an acid catalyst at a moderate temperature of 80 to 160°C (Lin, 1996; Pu and Shiraishi, 1993). Pu and Shiraishi (1993a; 1993b; 1994) did a variety of studies on wood liquefaction without a catalyst. The effects of liquefaction temperature, time, and phenol to wood ratio on liquefaction reaction were investigated. Although no acid catalyst was added, they reported that the liquefied products were found to be acidic, which was attributed to the likely formation of acetic acid during the liquefaction process (Pu and Shiraishi, 1993). Both strong acids (i.e., sulfuric acid and

hydrochloric acid) and weak acid (i.e., oxalic acid) can be used as a catalyst in wood liquefaction (Alma et al., 1995a; Alma et al., 1995b; Alma et al., 1998). Liquefied wood products using a strong acid catalyst can achieve higher combined phenol and lower wood residue content than that using a weak acid catalyst (Alma et al., 1995b; Alma et al., 1998; Lin, 1996). Novolac type liquefied wood resins can be directly synthesized from the co-condensation of liquefied wood and formaldehyde with an acid catalyst. The viscosity and the flow temperature of liquefied wood-phenol-formaldehyde (LWPF) resins are much lower than pure liquefied wood (Lin et al., 1995). The mechanical properties of compression molded products from LWPF resin are comparable to that of the conventional novolac resin (Alma et al., 1995b; Lin et al., 1995).

Despite these many advances in liquefaction technology, the mechanism of wood liquefaction has not yet been clearly understood due to the complicated structure and chemical composition of wood. Moreover, most previous studies on wood liquefaction have focused on completely converting wood into a liquid via a strong acid catalyst or high reagent solvent to wood ratios, which has resulted in a liquefaction process that is not economically favorable because special production equipments are required due to the high corrosiveness of the strong acids. Therefore, in our research on wood liquefaction we have focused on a process with a weak acid catalyst system. One significant difference of a weak acid catalyzed system to a strong acid system is the high wood residue content, which might not be desirable for most applications. However, in the development of novolac-type liquefied wood resins, liquefied wood residue can be utilized as filler in molded products, which present unique opportunity to enhance the economic feasibility of the new system. Thus, in this study, we focus on (1) characterization of liquefied wood residue from a weak acid catalyzed system, (2) examination of the properties of the novolac resin formulated from the liquefied wood, and (3) evaluation of the physical and mechanical properties of the compression molded products fabricated with the novolac resin.

Experimental

Preparation of liquefied wood and liquefied wood residues

Chinese tallow (*Triadica sebifera syn. Sapium sebiferum*) tree wood, collected as sawdust and reduced to fine particles of 20-200 mesh in a Wiley mill, was used in liquefaction. Phenol (90%, industrial grade) and wood were mixed at a 2/1 weight ratio with 5% (based on the amount of phenol) oxalic acid as a catalyst. Liquefaction temperature and time was 180°C and 90 min., respectively. Liquefaction reactions were conducted in two types of reactors: (1) 1L atmospheric three-neck glass reactor and (2) 1L sealed Parr Instrument Co. (Parr®) reactor. At the end of the liquefaction, the liquefied wood was cooled to room temperature to terminate the reaction. The liquefied wood was equally divided in two parts. One part was diluted with methanol and filtered with Whatman medium flow filter paper. The insoluble residues were oven dried at 105°C overnight, weighed, and the residue content as a percentage of the original wood was calculated. The dried wood residue was stored in a dessicator for subsequent characterization. The other part of the liquefied wood was used in the synthesis of the liquefied wood novolac resin.

Synthesis of liquefied wood/phenol/formaldehyde (LWPF) novolac resin

To prepare the novolac resin, the liquefied wood mixture was mixed with formaldehyde (36% concentration) at a phenol/formaldehyde molar ratio of 1/0.8 (phenol was based on the initially charged amount at liquefaction) and placed into the resin reactor. The additional oxalic acid (7% of phenol, w%) was added as a catalyst. The mixture was refluxed under continued stirring at 105°C for 80 min. At the end of the reaction time, the novolac resin was cooled down to room temperature and stored in the refrigerator before use.

Characterization of liquefied wood residue

The liquefied wood residues were characterized by chemical analysis, FT-IR spectroscopy, and X-ray diffraction analysis. The brief descriptions of the procedures are presented as follows:

Chemical analyses. The liquefied wood residues were first Soxhlet extracted to yield extractive-free materials in accordance with ASTM (American Society for Testing and Materials (ASTM), 1996b). Klason lignin (American Society for Testing and Materials, (ASTM), 1996c), holocellulose (American Society for Testing and Materials (ASTM), 1971a), and α-cellulose (American Society for Testing and Materials (ASTM), 1971b) were determined based on the extractive-free residues.

FT-IR spectroscopy. The FT-IR analysis of the liquefied wood residues was performed using a Nicolet Nexus 670 spectrometer equipped with a Thermo Nicolet Golden Gate MKII Single Reflection ATR accessory. A small amount of residue was directly applied on the diamond crystal.

X-ray diffraction analysis. The degree of crystallinity of the residues was measured by X-ray diffraction. The liquefied wood residues from different liquefaction conditions were pressed into disks and analyzed with a PANalytical X´pertPro Super X-ray diffractometer. The X-ray diffractograms were recorded from 0 to 40º at a scanning speed of 1º/s and sampling rate of 2 data/s. The crystallinity index (CrI) of the liquefied wood residue was calculated using the Segal method (Segal et al., 1959) per the following equation:

$$CrI(\%) = \frac{I_{002} - I_{am}}{I_{002}} \times 100 \qquad (1)$$

where I_{002} is the intensity of the diffraction from the (002) plane at 2θ=22.6º, and I_{am} is the intensity of the background scatter measured at 2θ=18.5º.

Characterization of LWPF novolac resin

Gel permeation chromatography (GPC).

The molecular weight and molecular weight distribution of the LWPF resin was determined by gel permeation chromatography (Waters Associates). The device was equipped with a differential refractometer detector and a Jordi Gel DVB Mixed Bed column. The resin samples were dissolved in 90/10 tetrahydrofuran (THF)/methanol solution. The same solvent was used as the mobile phase at a flow rate of 1.2 ml/min. The concentration of the sample was 2.5 mg/ml in THF/ methanol solution.

Differential scanning calorimetry (DSC)

The glass transition temperature (T_g) and the cure reaction of the LWPF resins were both performed on a TA DSC-Q100 calorimeter. To measure the T_g, about 10-15 mg of LWPF resin was put into an aluminum sample pan and sealed with a lid by crimping around the edge. The temperature of the DSC was programmed from ambient temperature to 250°C and back to 0°C at 20°C /min. to eliminate the effect of water that might exist in the samples. The samples were then heated again to 250°C at the same rate.

To study the cure kinetics, LWPF resin, hexamethyleneteramine (HMTA), and calcium hydroxide were homogeneously mixed at a weight ratio of 1:0.2:0.25. A small amount (10-15 mg) of the sample was placed in a high volume DSC sample pan that can withstand vapor pressure up to 10 MPa. Dynamic scans were conducted with four heating rates (5, 10, 15, and 20°C/min.) in a scanning temperature range from 25 to 200°C. The onset temperature (T_o) was determined from the DSC thermogram by drawing a tangent line from the inflection point to the baseline and recording the temperature at the intersection of these two lines.

Preparation of novolac moldings and evaluation of the performance of the molded panel

All novolac moldings were prepared with ingredient formula containing 37.7% LWPF novolac resin, 49.5% wood filler, 9.4% HMTA, 2.4% calcium hydroxide, and 1% zinc stearate. The same procedures described in a previous paper were used in fabricating the molding panels (Pan et al., 2005). Flexural and tensile test were performed using an Instron-4465 test machine in accordance with ASTM D-1037-96 (American Society for Testing and Materials (ASTM), 1996a). Forty eight hours soaking and 4 h boiling tests were performed to evaluate the dimensional stability of the molding panels.

Results and Discussion

Characterization of liquefied wood residue

Chemical analyses

Table 1 presents the average residue content of the liquefied wood and the average Klason lignin, holocellulose, and α-cellulose contents of the liquefied wood residue. The Klason lignin contents of both liquefied wood residues were lower than that of the original Chinese tallow tree wood (20.3%) (Eberhardt et al., 2007). The liquefied wood residue in the sealed system yielded a much higher Klason lignin content than the atmospheric system. Lignin is very susceptible to the liquefaction reaction and is the most reactive wood component during liquefaction.[2] However, degraded lignin has a tendency to undergo secondary condensation reactions (Kobayashi et al., 2004; Sarkanen, 1963). Pu and Shiraishi (1993) found that the Klason lignin content of liquefied wood residue gradually increase at lower P/W ratios with an increase in reaction time. Besides the re-condensation reaction of lignin, it was observed that the liquefied wood residue from the sealed system appeared to be much darker than that from the atmospheric system. This darker residue contained a significant portion of cinder-char type substance that could not been digested by sulfuric acid during the Klason lignin determination process. This formation of a cinder-char substance could also contribute to the higher Klason lignin content in the sealed

system. Furthermore, in the process of solvolysis during wood liquefaction, it is also possible that the phenol reacted with the dissolved lignin to form an insoluble new substance that was retained in the residue which in turn affected the Klason lignin determination.

Table 1. Residue content and chemical composition of liquefied wood residues.

	Residue content (%)	Klason lignin (%)	Holocellulose (%)	α -cellulose (%)
Atmospheric	70.06	9.16	81.25	54.09
Sealed	52.83	18.98	75.86	48.33

The holocellulose contents of the liquefied wood residues were consistent with their Klason lignin contents. In other words, the lower the Klason lignin content, the higher the holocellulose content. The α-cellulose content of the residues showed a similar trend as the holocellulose.

X-ray diffraction (XRD)

The X-ray crystallinity index (CrI) of the liquefied wood residues and the original tallow wood are listed in Table 2. In general, the CrI of the liquefied wood residue is higher than that of the original wood. This result was expected because part of the lignin was removed from the amorphous region of the liquefied wood residue during the liquefaction process (Table 1). It is important to note that the CrI is used to indicate the relative, rather than the absolute, amount of the crystalline region in cellulose (Ouajai and Shanks, 2005). Therefore, when the lignin in the amorphous region decreased, the relative portion of the crystalline region of cellulose increased. A similar result has also been found by other researchers (Trindade et al., 2005). Apparently, the CrI result of the liquefied wood residue is very consistent with the Klason lignin content of the liquefied wood residue (Table 1). The re-condensed lignin left on the residue from the sealed system very likely remained in an amorphous status so as to lower the relative percentage of the crystal region. In addition, the XRD results for the liquefied wood residue also provide a piece of supporting evidence for an explanation to a result in our previous study (Pan et al., 2005). Namely, the liquefaction rate of the three wood components is in a decreasing order of hemicellulose, lignin, amorphous cellulose, and crystalline cellulose. There is no clear evidence in this experiment of the liquefaction rate of hemicellulose. However, the lignin did undergo a faster liquefaction rate than the cellulose, thus, leaving the crystalline cellulose almost intact in the liquefied wood residue since the crystal structure in cellulose greatly limits the access to β-1,4-glycosidic bonds by reactants and catalysts (Zhao et al., 2006). Conversely, the amorphous part of cellulose is more readily accessible by water and other reactants (Vittadini et al., 2001).

Table 2. The X-ray crystallinity index (CrI, %) of the

	Tallow wood	Atmospheric	Sealed
CrI (%)	45.85	62.60	60.98

FT-IR spectroscopy

FT-IR spectra of woody materials are complex due to the various functional groups that exist in wood components and the complicated chemical environment of the wood components. Many peaks in wood IR spectra are broad and often overlap with neighboring peaks. However, the FT-IR spectra of the residues from atmospheric and sealed cooking systems did show some differences between each other and to that of the original wood (Fig. 1a).

The most obvious difference observed in the spectra was an intense absorbance at 1735 cm^{-1}, which occurred in the spectra of both the original wood and residues from the atmospheric liquefaction systems. It became a small shoulder or even disappeared (spectra not shown) in the spectra of residues from the sealed liquefaction systems, indicating different liquefaction reactions from a pressurized metal reactor versus atmospheric glass reactor. It is known that the absorption bands from 1710 to 1740 cm^{-1} mainly arose from the carbonyl (C=O) stretch in unconjugated ketone, ester, or carboxylic groups in carbohydrates and not from lignin (Hoareau et al., 2004; Schwanninger et al., 2004). It is also shown that carbonyl groups occur abundantly with the methyl and acetyl ester groups in pectin, the acetyl ester groups in xylan, and in the oxidative products of cellulose (Bjarnestad and Dahlman, 2002; Lojewska et al., 2005; Sun et al., 1998). However, the wood species used in this experiment, Chinese tallow tree (*Triadica sebifera* syn. *Sapium sebiferum*), is not rich in pectin (American Society for Testing and Materials (ASTM), 1996a), and the most profound effects of cellulose oxidation occurred at 250°C (Lojewska et al., 2005), which is far beyond the temperature used in this experiment. Consequently, the absorbance band at 1735 cm^{-1} in the spectra in this experiment is most likely attributed to the ester carbonyl group in xylan. The phenomenon of the disappearance of the 1735 cm^{-1} band in the spectra of the residue from the Parr® reactor is very similar to that of the wood or other natural cellulosic fiber treated with sodium hydroxide (NaOH) (Mwaikambo and Ansell, 2002; Sun et al., 2004). This phenomenon occurred in alkali-treated natural fibers has been interpreted as the hydrolysis of the ester linkages in xylan (Cyran et al., 2004.). Xylans are closely associated with other plant cell wall constituents, such as lignin and pectic polysaccharides, by ferulic acid or uronic acid through ester linkages (Kacurakova et al., 1999; Sun et al., 1998). In the presence of alkalis, the hydroxyl ions cause the saponification of these ester linkages and "peel off" the hemicellulose from the adjacent lignin or cellulose molecules into the solution (Sun et al., 1999; Xu et al., 2006).

Compared to the reaction conditions of the atmospheric liquefaction in the three neck flask, the disappearance of peak 1735 cm^{-1} in the sealed Parr® reactor system could be due to the pressurized effect or the catalytic effect of the elements associated with the internal lining of the Parr® reactor during the liquefaction process. To explore these two possible effects, a reaction of wood liquefaction was conducted in a sealed glass tube under the same conditions used in the liquefaction in a Parr® reactor. Fig. 1b shows the spectrum of the LWR from three different reactors (i.e., a sealed glass tube, a Parr® reactor, and a three neck flask reactor). By comparison of spectrum A (sealed glass tube) and spectrum C (a three neck flask reactor), the similarity of a strong absorbance at 1735 cm^{-1} in both spectra indicates that the effect of pressure was not the cause of the breaking of the carbonyl bonds in the hemicellulose. Therefore, the catalytic effects of some metal elements associated

with the Parr® reactor is likely the main reason that caused the breaking of the ester carbonyl bonds in the hemicellulose during the liquefaction process.

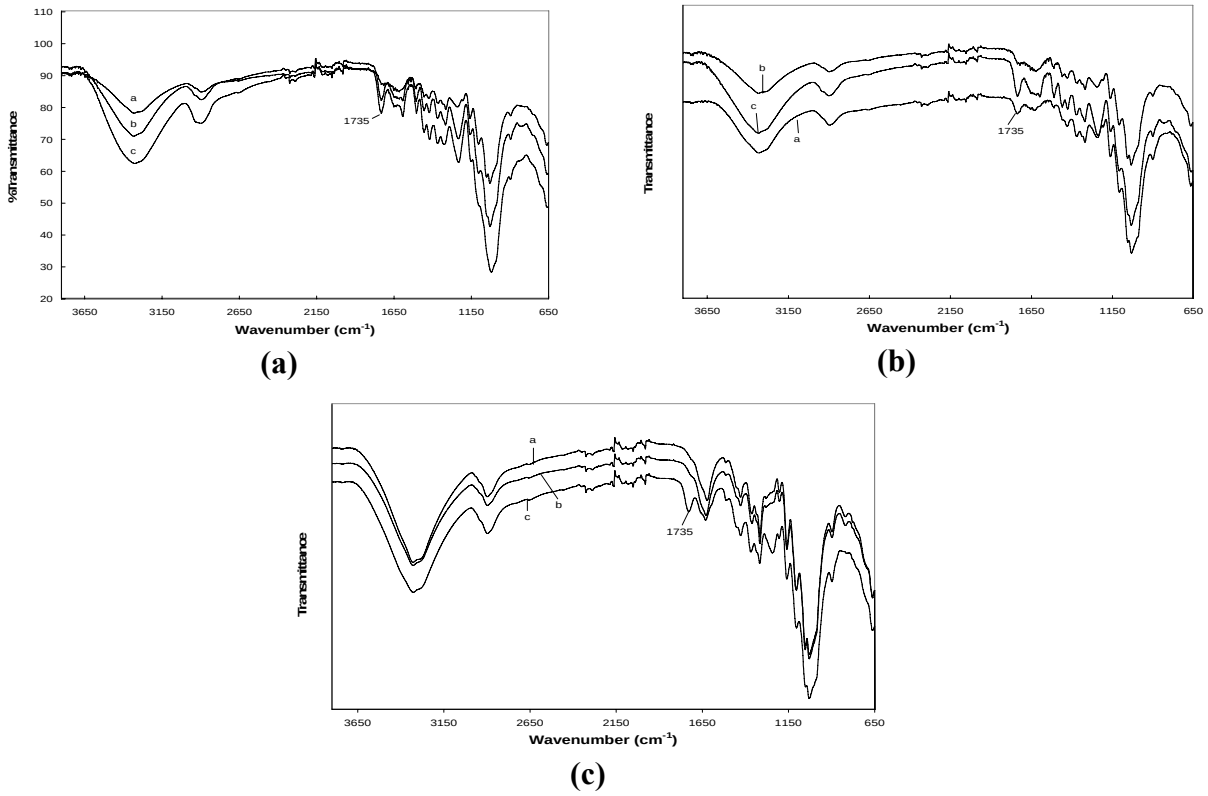

Fig. 1. FT-IR spectra of residues from (a) atmospheric (spectrum a), sealed cooking (spectrum b), and untreated wood (spectrum c); (b) sealed glass tubing reactor (spectrum a), Parr reactor (spectrum b), and three neck flask (spectrum c); (c) sealed glass tubing reactor with the addition of $FeCl_2$ (spectrum a), $FeCl_3$ (spectrum b) and untreated tallow wood particles (spectrum c). P/W ratio was 1/1 and liquefaction temperature was 150°C

The Parr® reactor used in this experiment was made from stainless steel T316. The composition of T316 is iron (65%), nickel (12%), chromium (17%), molybdenum (2.5%), manganese (2%), and silicon (1%) (Parr Instrument Co., 2006.). It is well known that iron can be easily oxidized to Fe^{2+} or Fe^{3+} ions under acidic conditions, which was the condition used in this experiment. In addition, iron is more active than most other metal elements present in the Parr® reactor, and it constitutes the major element in T316 stainless steel. Therefore, it is postulated that Fe^{2+} and/or Fe^{3+} ions were the possible catalysts that helped to break the ester bond in xylan. Thus, a further experiment of wood liquefaction was conducted with the addition of a small amount of $FeCl_2$ or $FeCl_3$ in a sealed glass tube. Fig. 1c shows the FT-IR spectra of the LWR with the addition of iron additives and untreated tallow wood particles. It can be seen that the 1735 cm^{-1} peak disappeared in the spectra of LWR with $FeCl_2$ and $FeCl_3$. Based on the above results, it is very likely that Fe^{2+} and/or Fe^{3+} ions released from the internal walls of the Parr® reactor helped to break down the ester carbonyl bond in the xylan during the acidic wood liquefaction reaction and caused the differences in the FT-IR spectra between the liquefied wood residue from the Parr®

reactor and the three neck flask. Some researchers have reported that some transition metals, especially iron species, can be used as redox catalysts in the pyrolysis of brown coal and the oxidation of phenol (Calleja et al., 2005; Domazetis et al., 2006). However, no research on the catalytic effect of iron ions on wood liquefaction has been reported yet. Further study is needed to study this possibility.

Properties of novolac resin made with liquefied wood

Gel permeation chromatography

The number-average molecular weight (Mn), weight-average molecular weight (Mw), polydispersity (Mw/Mn) of of the novolac resin made with the liquefied wood prepared from the sealed system (LWPF-A) were significantly higher than that of the resin made with the liquefied wood from the atmospheric system (LWPF-B) (Table 3). It is interesting to note that the Mw and Mw/Mn of LWPF-A are 15 and 7 times, respectively, higher than those of LWPF-B. In general, the Mw is sensitive to the admixture of molecules of high molecular mass while the Mn is sensitive to the admixture of molecules of low molecular mass.[38] As shown in Fig. 2, LWPF-A resin consists of a large high molecular weight fraction as compared to that of LWPF-B, indicating that LWPF-A is highly advanced and

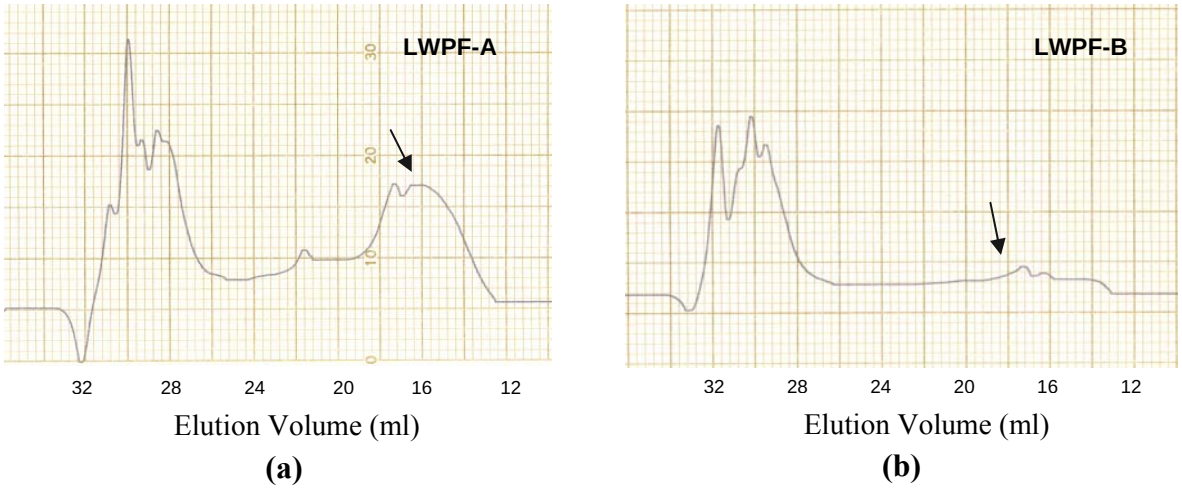

Fig. 2. GPC chromatograms of (a) LWPF-A and (b) LWPF-B resins (Arrows indicate high molecular weight fraction).

polymerized with a branched network. Furthermore, it is also generally recognized that the molecular characteristic (i.e., molecular weight and its distribution, and degree of polymerization) of the resin is one of the most important properties relating to the overall applications and performances of the resin adhesive. Many resin properties such as solubility, mobility, rate of curing, and the strength and durability of the compression molded products are significantly affected by molecular characteristics of the resin. In view of the substantial differences in the molecular weight distribution of the two LWPF novolac resins, further in depth investigations of the resin systems is highly desirable.

Currently, these two LWPF resins are being fractionated by a preparative GPC column. The low and high molecular weight fractions will be collected and analyzed by NMR and mass spectroscopy.

Differential scanning calorimetry

Table 3 shows that the glass transition temperature (T_g) of the LWPF-A resins (64.02°C) was approximately 15 °C higher than that of LWPF-B resin (50.15°C), which largely corresponded with their molecular weight. In other words, the resin that had a higher molecular weight, in general, had a higher glass transition temperature.

The dynamic DSC curves of the two LWPF resins at different heating rates are shown in Fig. 3. As expected, the onset temperature (T_o) and peak temperature (T_p) of both resins shifted to higher temperatures with an increased heating rate. It is noted that LWPF-A resin had slightly higher T_o and lower T_p, respectively, as compared to that of LWPF-B resin (Table 3)**.**

Table 3. Molecular weight composition and T_g of the LWPF resins.

	Molecular weight			Tg [a] (°C)	To[b] (°C)	Tp[c] (°C)
	Mn	Mw	Mw/Mn			
LWPF-A	1575	22012	13.98	64.02	115.8	128.7
LWPF-B	662	1418	2.14	50.15	113.3	129.9

[a]glass transition temperature
[b]onset cure temperature, extrapolated values from the intercepts of the onset temperature vs. heating rate plot.
[c]peak cure temperature, extrapolated values from the intercepts of the peak temperature vs. heating rate plot.

The activation energies of the LWPF resin were calculated by the Kissinger method (Kissinger, 1957.). The Kissinger equation is expressed as follows:

$$\ln\left(\frac{\phi}{T_p^2}\right) = -\frac{E}{R}\cdot\frac{1}{T_p} + \ln\left(\frac{RA}{E}\right) \tag{3}$$

where Φ is the heating rate (K/s), T_p is the peak temperature (K) at the given heating rate, and R is the gas constant. The activation energy (E) can be obtained by linear regression from Equation 3. Based on this method, the activation energies of the LWPF-A and LWPF-B were 96.55 and 97.54 KJ/mol, respectively. The activation energy is the energy that must be provided to enable the reactants to react. In general, lower activation energy indicates that the reaction proceeds faster at a given temperature. LWPF-A resin showed a slightly lower activation energy than LWPF-B resin, indicating that it also cures faster than LWPF-B resin under the same temperature. It should be mentioned that the activation energies of the LWPF resin obtained in the study were higher than the typical PF resins as reported by other researchers (Alonso et al., 2004; American Society for Testing and Materials (ASTM), 1971b), but close to that of a lignin-phenol-formaldehyde resin (Alonso et al., 2004).

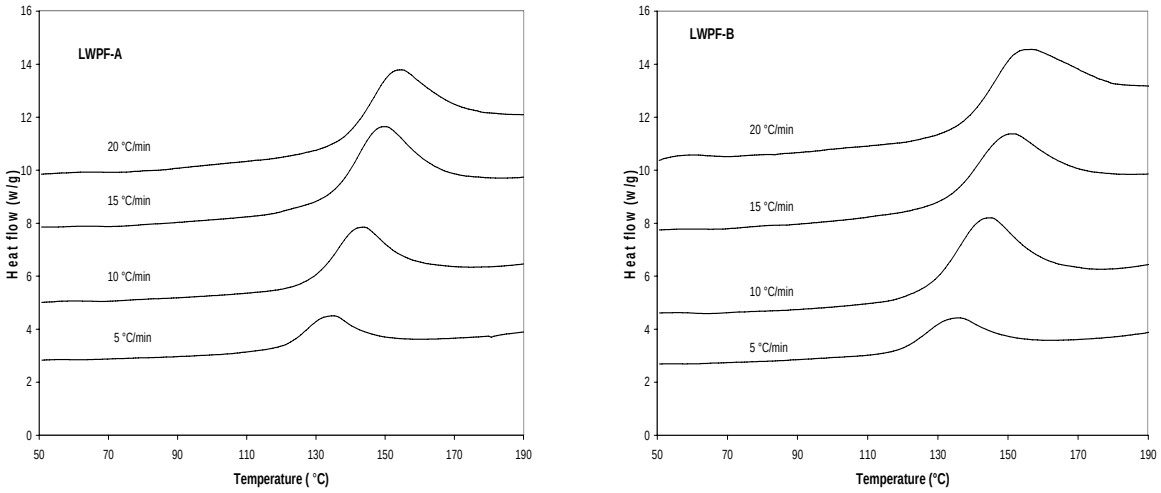

Fig. 3. Dynamic DSC curves of (a) LWPF-A and (b) LWPF-B resins

Physical and mechanical properties of the novolac moldings

Table 4 presents the physical and mechanical properties of the novolac compression moldings from the LWPF resins. The moldings from LWPF-A resin gave better results than LWPF-B resin both in the flexural and tensile tests and provided substantially better dimensional stability. This is rather expected because with a higher molecular weight and a shorter cure time, LWPF-A resin had favorable properties to attain highly effective cross-linking than LWPF-B resin during the cure process, which in turn resulted in the better physical and mechanical properties.

Table 4. Bonding properties of the LWPF resins

	Flexural Strength (psi)		Tensile Strength (psi)		Thickness Swelling (%)	
	MOR	MOE	MOR	MOE	48 h soaking	4 h boiling
LWPF-A	10,300	1,252,251	7,369	645,473	5.09	19.23
LWPF-B	8,890	1,131,397	6,203	625,624	6.55	25.95

Conclusions

Wood liquefaction conducted in an atmospheric glass reactor and a sealed Parr® reactor underwent different reaction mechanisms. Lignin is very susceptible to the liquefaction reaction; however, it also underwent a recondensation reaction. The holocellulose and α-cellulose contents of the residues were consistent with the Klason lignin content. The FT-IR spectra of the liquefied wood residues implied that the iron ions (Fe^{2+} and Fe^{3+}) have catalytic effects to break the ester carbonyl bond in xylan during the liquefaction reaction. The CrI of liquefied wood residue was greater than the original wood particles, indicating that lignin undergoes a faster liquefaction rate than crystalline cellulose. The LWPF novolac resin made with liquefied wood in the atmospheric system (i.e., LWPF-A) obtained higher polymerization than that from the sealed liquefaction system (i.e., LWPF-B). The

onset cure temperature of LWPF-A resin was slightly higher than LWPF-B. The activation energies of LWPF-A resin was slightly higher than LWPF-B and were similar to a lignin-phenol-formaldehyde resin, however, they were higher than a typical phenol-formaldehyde resin. The compression molded panels made with LWPF-A resin provided better physical and mechanical properties than the panels that made with LWPF-B resin.

References

Alma, M.H., Yoshioka, M., Yao, Y., and Shiraishi, N. 1995a. Some characterizations of hydrochloric acid catalyzed phenolated wood-based materials. Mokuzai Gakkaishi 41(8): 741-748.

Alma, M.H., Yoshioka, M., Yao, Y., and Shiraishi, N. 1995b. Preparation of oxalic acid catalyzed resinified phenolated wood and its characterization. Mokuzai Gakkaishi 41(12): 1122-1131

Alma, M.H., Yoshioka, M., Yao, Y., and Shiraishi, N. 1998. Preparation of sulfuric acid catalyzed phenolated wood resin. Wood Sci. Technol. 32: 297-308.

Alonso, M.V., Oliet, M., Perez, J.M., Rodriguez, F., and Echevrria, J. 2004. Determination of curing kinetic parameters of lignin-phenol-formaldehyde resol resins by several dynamic differential scanning calorimetry methods. Thermochim Acta 419: 161-167

American Society for Testing and Materials (ASTM). 1996a. Standard test method for evaluating properties of wood-base fiber and particle panel materials. ASTM D 1037-96.

American Society for Testing and Materials (ASTM). 1996b. Standard test method for preparation of extractive-free wood. ASTM D 1105-96

American Society for Testing and Materials (ASTM). 1996c. Standard test method for acid-insoluble lignin in wood. ASTM D 1106-96.

American Society for Testing and Materials (ASTM). 1971a. Standard method of test for holocellulose in wood. ASTM D 1104-56.

American Society for Testing and Materials (ASTM). 1971b. Standard method of test for α-cellulose in wood. ASTM D 1103-60.

Bjarnestad, S., and Dahlman, O. 2002. Chemical compositions of hardwood and softwood pulps employing photoacoustic Fourier transform infrared spectroscopy in combination with partial least-squares analysis. Anal. Chem. 74: 5851-5858.

Calleja, G., Melero, J.A., Martinez, F., and Molina, R. 2005. Activity and resistance of iron-containing amorphous, zeolitic and mesostructured materials for wet peroxide oxidation of phenol. Water Res. 39:1741-1750.

Cyran, M., Courtin, C.M., and Delcour, J.A. 2004. Heterogeneity in the fine structure of alkali-extractable arabinoxylans isolated from two rye flours with high and low breadmaking quality and their coexistence with other cell wall components. J. Agric. Food. Chem. 52: 2671-2680.

Domazetis, M., Raoarun, M., and James, B.D. 2006. Low-temperature pyrolysis of brown coal containing iron hydroxyl complexes. Energy Fuels 20:1997-2007.

Eberhardt, T.L., Li, X., Shupe, T.F., and Hse, C.Y. 2007. Chinese tallow tree utilization: characterization of extractives and cell wall chemistry. Wood Fiber Sci. in press.

Hoareau, W., Trindade, W.G., Siegmund, B., Castellan, A., and Frolini, E. 2004. Sugar cane bagasse and curaua lignins oxidatized by chlorine dioxide and reacted with furfuryl alcohol: characterization and stability. Polym. Degrad. Stab. 86: 567-576.

Kacurakova, M., Wellner, N., Ebringerova, A., Hromadkova, Z., Wilson, R.H., and Belton, P.S. 1999. Characterization of xylan-type polysaccharides and associated cell wall components by FT-IR and FT-Raman spectroscopies. Food Hydrocolloids 13: 35-41.

Kissinger, H.E. 1957. Reaction kinetics in differential thermal analysis. Anal. Chem. 29: 1702-1706.

K Kobayashi, M., Asano, T., Kajiyama, M., and Tomita, B. 2004. Analysis on residue formation during wood liquefaction with polyhydric alcohol. J. Wood Sci. 50: 407-414.

Lei, Y., Wu, Q., and Lian, K. 2006. Cure kinetics of aqueous phenol-formaldehyde resins used for oriented strandboard manufacturing: analytical technique. J. Appl. Polym. Sci. 100: 1642-1650.

Lin, L.Z. 1996. Characterization of phenolated wood and study on the liquefaction mechanism of lignin. Ph.D dissertation, Kyoto University.

Lin, L., Yoshioka, M., Yao, Y., and Shiraishi, N. 1995. Preparation and properties of phenolated wood/phenol/formaldehyde cocondensed resin. J. Appl. Polym. Sci. 58: 1297-1304.

Lojewska, J., Miskowiec, P., Lojewski, P., and Proniewicz, L.M. 2005. Cellulose oxidative and hydrolytic degradation: In situ FTIR approach. Polym. Degrad. Stab. 88: 512-520.

McCrum, N.G., Buckley, C.P., and Bucknall, C.B. 1992. Principles of polymer engineering. Oxford University Press, London, p 9.

Mwaikambo, L.Y., and Ansell, M.P. 2002. Chemical modification of hemp, sisal, jute, and kapok fibers by alkalization. J. Appl. Polym. Sci. 84:2222-2234.

Ouajai, S., and Shanks, R.A. 2005. Composition, structure and thermal degradation of hemp cellulose after chemical treatments. Polym. Degrad. Stab. 89: 327-335.

Parr Instrument Co. 2006. http://www.parrinst.com/default.cfm?page_id=107

Pan, H., Shupe, T.F., and Hse, C.Y. 2005. Preliminary investigation of bio-composites fabricated from liquefied wood-phenol-formaldehyde co-condensed resin. In Wood Adhesive 2005, Frihart, C.R. Ed. Forest Products Society, San Diego, 2005.

Pu, S., and Shiraishi, N. 1993. Liquefaction of wood without a catalyst I. time course of wood liquefaction with phenols and effects of wood/phenol ratios. Mokuzai Gakkaishi 39(4): 446-452.

Pu, S., and Shiraishi, N. 1993. Liquefaction of wood without a catalyst II. Weight loss by gasification during wood liquefaction, and effects of temperature and water. Mokuzai Gakkaishi 39(4): 453-458.

Pu, S.,and Shiraishi, N. 1994. Liquefaction of wood without a catalyst IV. Effect of additives, such as acid, salt, and neutral organic solvent. Mokuzai Gakkaishi 40(8): 824-829.

Sarkanen, K.V. 1963. In Wood Chemistry, Browning, B. L., Ed.; Interscience publisher: New York, Chap. 5.

Segal, L., Creely, J.J., Martin, A.E., and Conrad, C.M. 1959. An empirical method for estimating the degree of crystallinity of native cellulose using the X-ray diffractometer. Textile Res J. 29: 786-794.

Schwanninger, M., Rodrigues, J.C., Pereira, H., and Hinterstoisser, B. 2004. Effects of short-time vibratory ball milling on the shape of FT-IR spectra of wood and cellulose. Vib Spectrosc. 36: 23-40.

Sun, J.X., Mao, F.C., Sun, X.F., and Sun, R.C. 2004. Comparative study of hemicelluloses isolated with alkaline peroxide from lignocellulosic materials. J. Wood Chem. Technol. 24: 239-262.

Sun, R.C., Fang, J.M., Goodwin, A., Lawther, J.M., and Bolton, A.J. 1998. Factionation and characterization of polysaccharides from abaca fiber. Carbohydr. Polym. 37: 351-359.

Sun, R.C., Fang, J.M., Rowlands, P., and Bolton, J. 1998. Physicochemical and thermal characterization of wheat straw hemicelluloses and cellulose. J. Agric. Food Chem. 46: 2804-2809.

Sun, R.C., and Hughes, S. 1999. Fractional isolation and physic-chemical characterization of alkali-soluble polysaccharides from sugar beet pulp. Carbohydr .Polym. 38: 273-281.

Trindade, W.G., Hoareau, W., Megiatto, J.D., Razera, A.T., Castellan, A., and Frollini, E. 2005. Biomacromolecules 6: 2485-2496.

Vittadini, E., Dickinson, L.C., and Chinachoti, P.C. 2001. ^{1}H and ^{2}H NMR mobility in cellulose. Carbohydr. Polym. 46: 49-57.

Xu, F., Sun, J.X., Liu, C.F., and Sun, R.C. 2006. Comparative study of alkali- and acidic organic solvent-soluble hemicellulosic polysaccharides from sugarcane bagasse. Carbohydr. Res. 341: 253-261.

Zhao, H., Kwak, J.H., Wang, Y., Franz, J A., White, J.M., and Holladay, J.E. 2006. Effects of crystallinity on dilute acid hydrolysis of cellulose by cellulose ball-milling study. Energy Fuels 20: 807-811.

Advanced Biomass Science and Technology for Bio-Based Products

Editors
Chung-Yun Hse, Zehui Jiang, and Mon-Lin Kuo

Associate Editors
Feng Fu and Paul Y. Burns

Developed from a symposium sponsored by:
Chinese Academy of Forestry & USDA Forest Service, Southern Research Station

May 23-25, 2007
Beijing, China

Printed in the People' s Republic of China.